PS Geologically Realistic Fluvial Point Bar Geocellular Models: Conditioning Algorithms with Outcrop Statistics*

Andrew L. McCarthy[1], Lisa Stright[1], Paul R. Durkin[2], and Stephen Hubbard[3]

Search and Discovery Article #42283 (2018)**
Posted October 1, 2018

*Adapted from poster presentation given at 2018 AAPG Annual Convention & Exhibition, Salt Lake City, Utah, May 20-23, 2018
 DOI:10.1306/42283McCarthy2018

[1]Geosciences, Colorado State University, Fort Collins, Colorado, United States (andrew.mccarthy@colostate.edu)
[2]Geological Sciences, University of Manitoba, Winnipeg, Manitoba, Canada
[3]Geoscience, University of Calgary, Calgary, Alberta, Canada

Abstract

Geostatistical reservoir modeling necessitates assumptions that often over-simplify heterogeneity, causing realizations to belie complex geologic reality. Outcrop studies provide robust suites of subseismic-scale (bed- to geobody-scale) statistics that characterize internal geobody architecture (e.g., bed thicknesses and lengths, grain size distributions). However, direct integration of such data into subsurface modeling workflows that capture geological complexity, remains challenging. This study: (1) presents bed-scale statistics from Late Cretaceous Horseshoe Canyon Formation fluvial point bar deposits that outcrop in southeastern Alberta, (2) investigates multiple modeling methodologies to test how different algorithms can integrate such statistics into reservoir modeling workflows, and (3) generates models that retain the geological essence of the outcrop deposits.

Stratigraphic sections (n = 40) record grain size, sedimentary structures, and bedding characteristics, providing the basis for reservoir model facies classification. Differential GPS surveys delineate individual lateral accretion packages (LAPs), capturing the stratigraphic framework for modeling outcrop architecture. Vertical and horizontal facies proportions and transition probabilities are calculated from measured sections, and constrain the probability that a facies is present at specific stratigraphic positions within each LAP. Bed-scale correlations are crucial for robust characterization of outcrop heterogeneity with such statistics. Probability cubes derived from these outcrop statistics guide simulations. Nested Truncated Gaussian Simulation (nTGS) is compared with Plurigaussian Simulation (PGS). nTGS realizations produce geologically-realistic outcomes with a small loss of fidelity to input facies proportions. PGS realizations produce less-geologically-realistic realizations, but better-preserve global facies proportions. Neither reproduces the LAP internal architecture observed in outcrop. Training images derived from outcrop statistics for multiple-point simulation achieve what nTGS and PGS could not, generating models with a better visual match to the outcrop that honors input statistics. This study presents a pathway to directly constrain models to measured outcrop statistics while also reproducing visual outcrop heterogeneity. As such, flow simulations on such models will test the flow-impacts of outcrop-derived architecture rather than purely stochastic heterogeneity.

1. Objectives

Build bed-scale models that:

1) Honor bed-scale outcrop statistics
   - Global Proportions and NTG Trends
   - Vertical Facies Proportion Curves
   - Facies Transitions
   - Bed thicknesses and lengths (indirectly)

2) Employ readily available, “off the shelf” algorithms:
   - Sequential Indicator (SIS)
   - Co-Sequential Indicator (COSIS)
   - Truncated Gaussian (TGS)
   - Plurigaussian (PGS)
   - Multiple-Point (MPS)

3) Reproduce a given geologic conceptual model (visual essence of the outcrop)

4) Produce realizations that can test impact of bed-scale detail on inter- and intra- point bar connectivity and flow.

2. Geologic Background

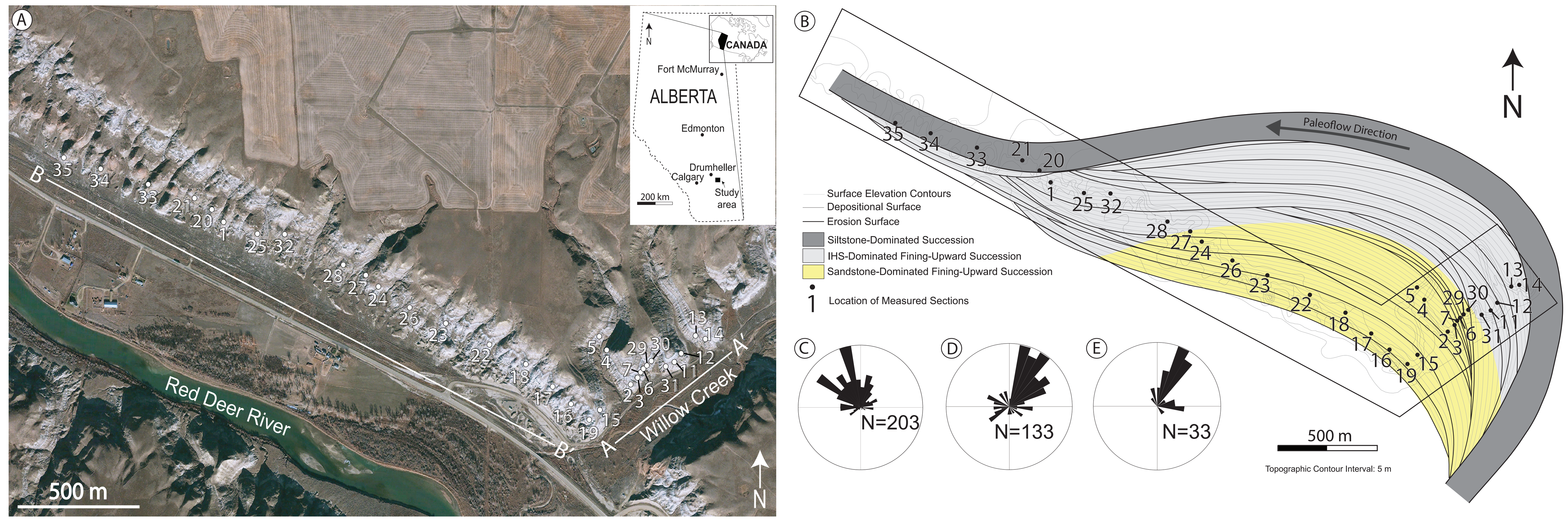

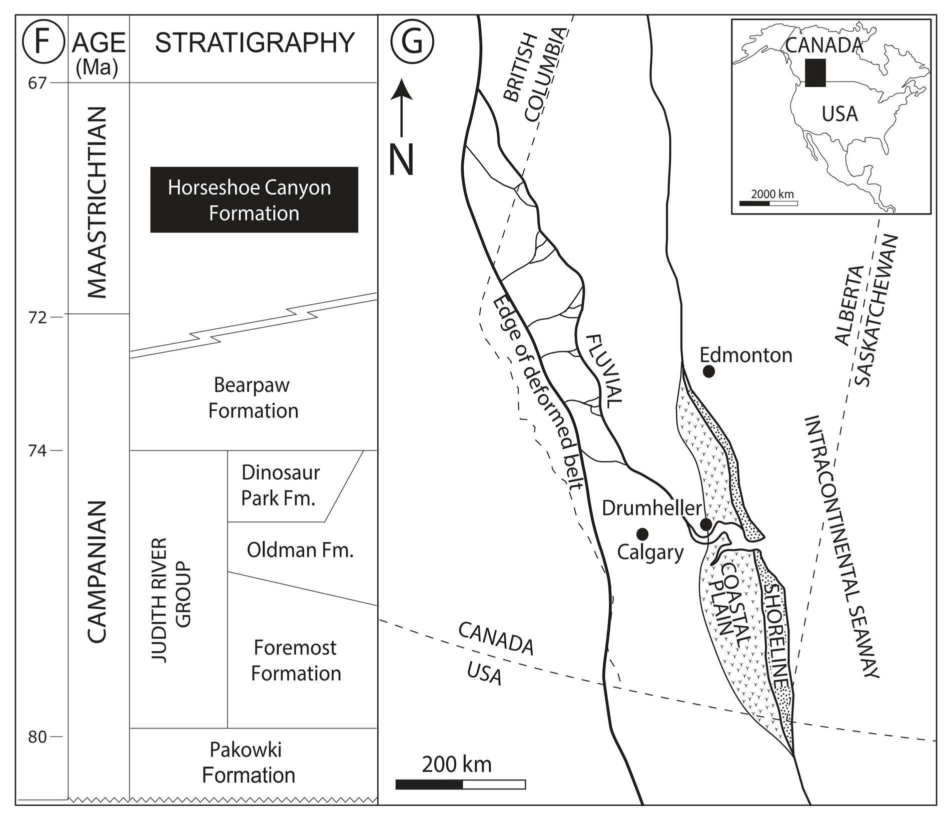

Figure 2.1: A) Satellite image (Google, 2016 - DigitalGlobe) of outcrops in the Red Deer River valley with measured sections locations. Study location shown on inset. B) Map-view interpretation of the point bar and associated abandoned channel deposits. Lateral accretion package migration direction varies through time, and deposits become more fine-grained from upstream to downstream. C) Paleoflow measurements (trough-cross stratification and clast imbrication) D) Depositional surfaces dip direction. E) Erosion surfaces dip direction. F) Stratigraphic Column for Horseshoecanyon Formation. G) Paleogeographic reconstruction of WCSB for Horseshoe Canyon Formation time (Modified from Leckie and Smith, 1992). Inset map shows location in North America. (Modfied from Durkin et al., 2016)

Horseshoe Canyon Formation outcrops exposed at Red Deer river valley in central Alberta comprise a 12-16 m thick fluvial meander belt deposit, which unconformably overlies shorefaces sands, and is capped by a laterally extensive coal (Ainsworth et al., 2015). Sediments shed off a NW-SE orogenic front were transported by rivers east and south until they were deposited at the margin of the Cretaceous Western Interior Seaway as part of Western Canada Sedimentary Basin (WCSB) fill. Outcrops are well-exposed due to “badlands” style topography 12 km southeast of Drumheller, AB. A 3 km NW-SE (“Red Deer River”) exposes successions roughly parallel to flow direction, and a 1 km NE-SW transect (“Willow Creek”) exposes successions roughly orthogonal to flow direction.

3. Stratigraphy and Zone Architecture

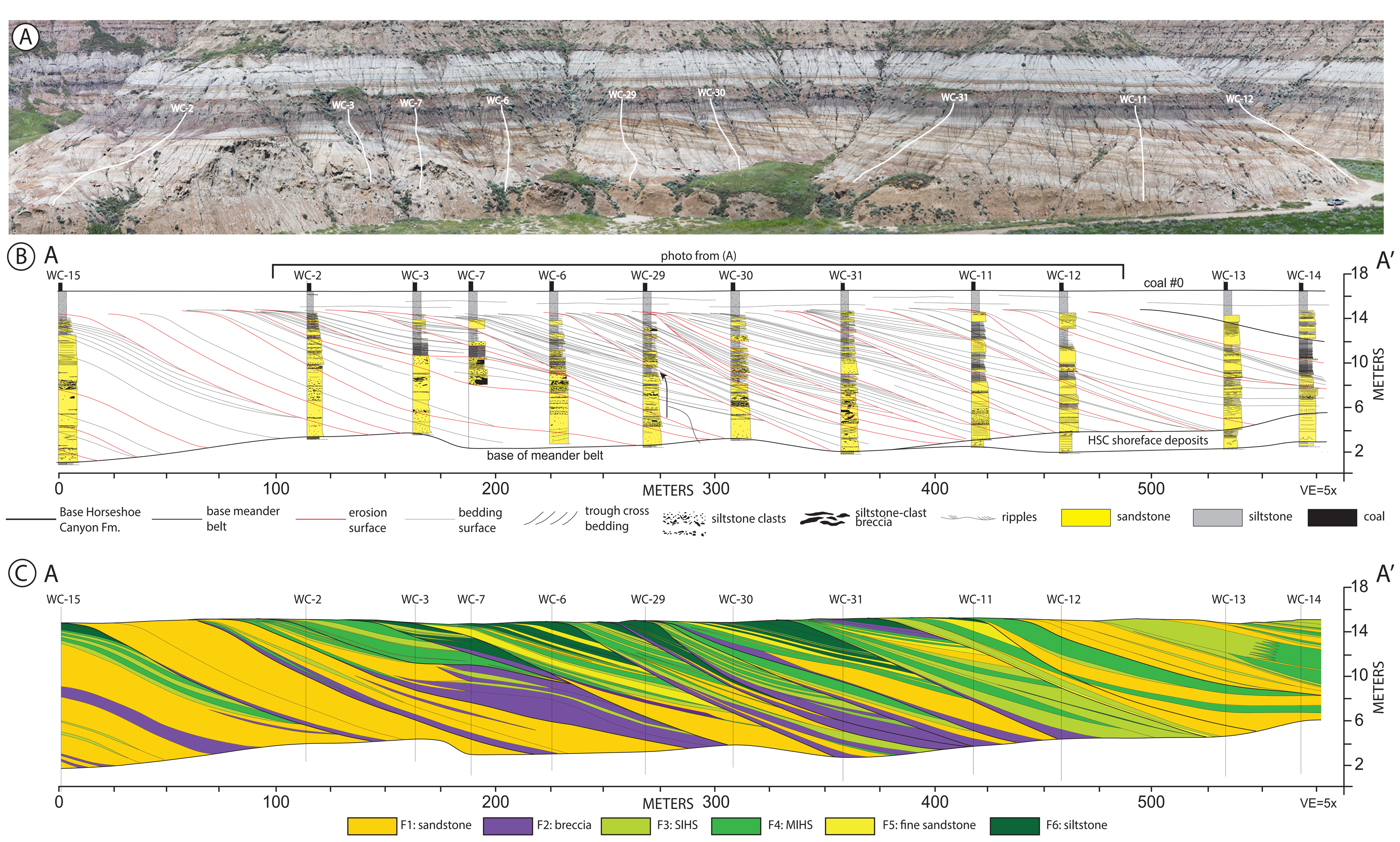

Figure 3.1: A) Willow Creek outcrop photomosaic with indicated section locations. B) Cross sections of all measured sections from Willow Creek oriented in the depositional dip direction. B) Field observations and photomosaic analysis. C) Corresponding facies correlation (Modified from Durkin et al., 2016).

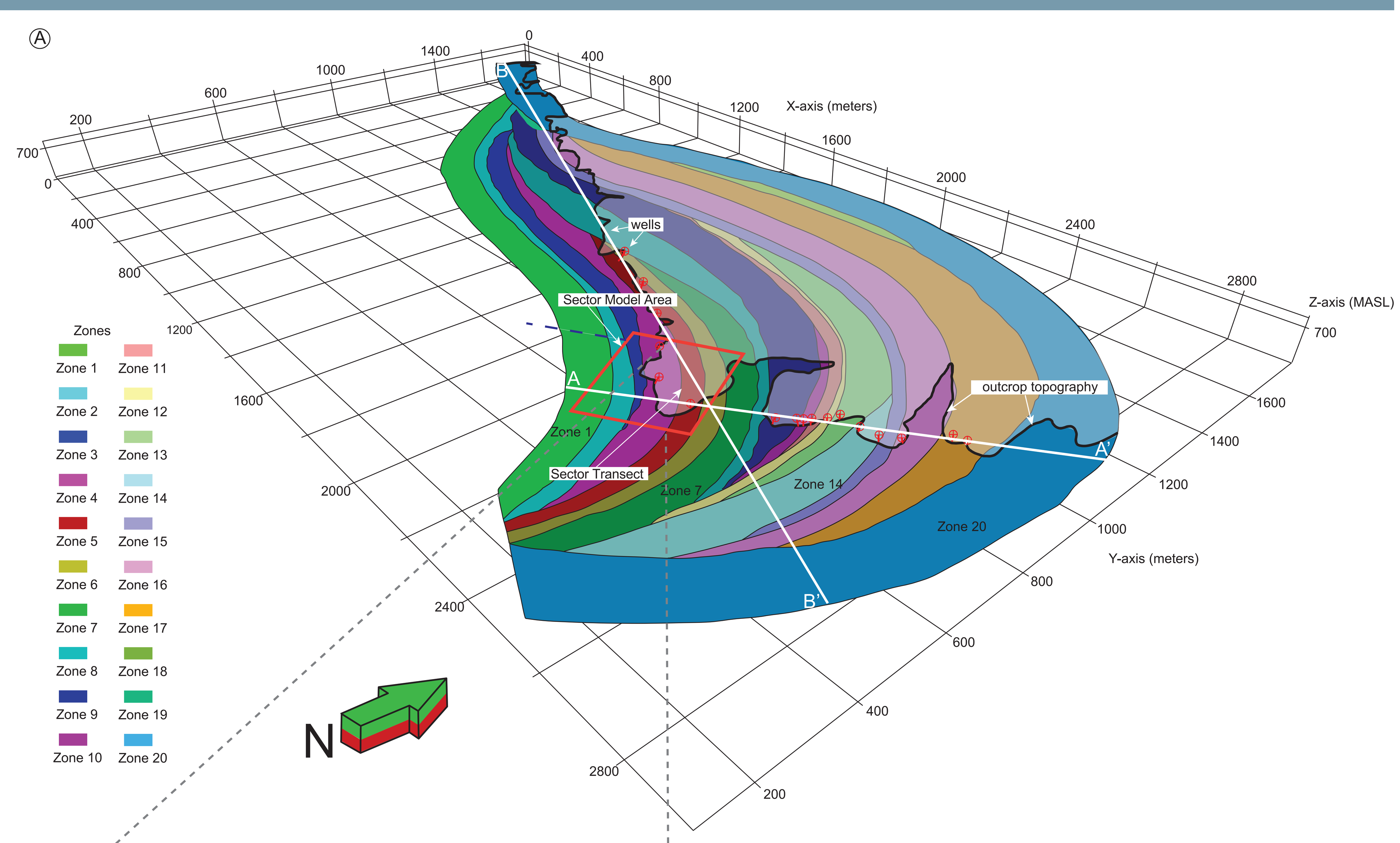

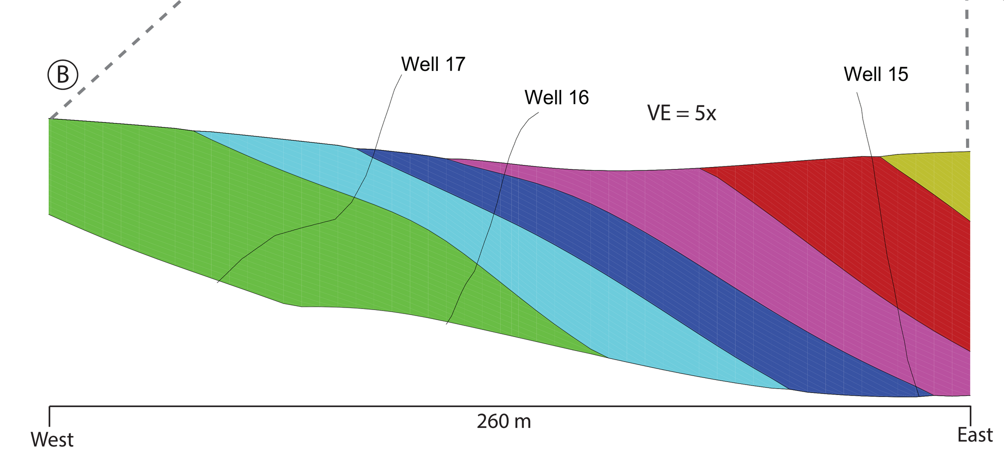

Figure 3.2: A) Zone architecture of the geocellular model. Locations of the Willow Creek cross-section and measured-section “pseudo-wells” are indicated. The small sector model taken for Plurigaussian testing and transect for visualization are also labeled. B) The sector transect inspects six LAP Zones. (Modified from Durkin et al., 2016).

Steeply dipping intra-point bar erosion surfaces that truncate underlying strata characterize the stratigraphic architecture of the deposits. Sigmoidal erosion surfaces bound concordantly-bedded lateral accretion packages (LAP) of consistent dip direction and magnitude. The stratigraphic framework and facies of Durkin et al. (2015) are used as the basis for this study. High-energy facies include sandstone (F1), siltstone-clast brecca (F2), and sandstone with siltstone and organic interbeds (SIHS; F3). Moderate-energy facies include siltstone with sandstone and organic interbeds (MIHS; F4) and very fine to fine-grained sandstone with ripples (F5). Siltstone (F6) records low-energy suspension settling of sediment. Planform reconstructions of the meander bend architecture reveal a complex history of point bar accretion with punctuated rotation events and ultimate channel abandonment.

The constructed 3D geocellular model has a grid cell size of 5 m x 5 m x 0.3 m (x, y, z) to represent fine-scale heterogeneity. Zones were defined by intra-point bar erosion surfaces that demarcate LAPs. Zone layers (parallel to sigmoidal surfaces) are 0.3 m thick so as to capture outcrop detail without compromising computational ability. Measured sections were integrated as hard-data for simulation as “pseudo” wellbores. TGS facies simulations were run on this grid. A sector model was taken out of the original grid to assess other simulation methods. Trends within packages and across zones make this an ideal dataset to test fine-scale facies simulation.

Geologically Realistic Fluvial Point Bar Geocellular Models: Conditioning Algorithms With Outcrop Statistics

Andrew L. McCarthy[1] (Andrew.McCarthy@colostate.edu) Cell: 626-390-1439
Lisa Stright[1], Paul R. Durkin[2], Stephen M. Hubbard[3]
[1]Department of Geosciences, Colorado State University, [2]Department of Geological Sciences, University of Manitoba, [3]Department of Geosciences, University of Calgary

4. Statistical Methods & Probability Volume

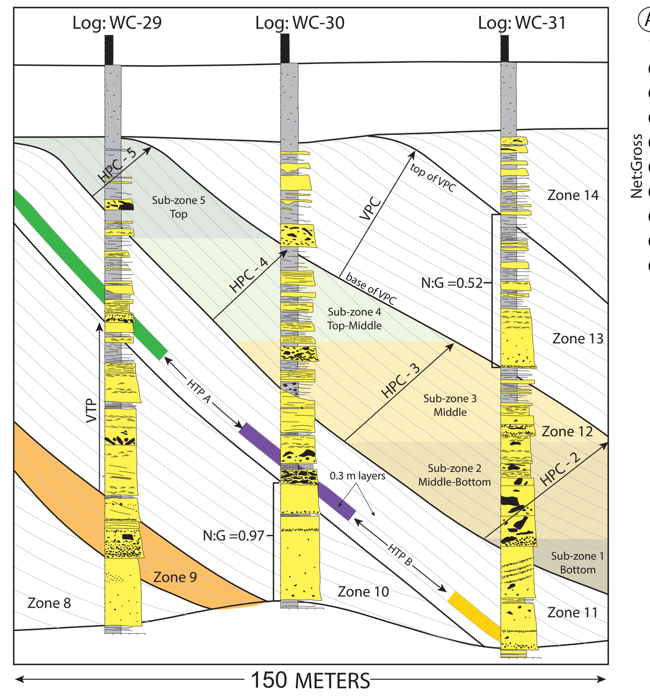

Figure 4.1: A) Willow Creek measured sections indicating key statistical parameters and stratigraphic architecture. (Modified from Durkin et al., 2016)

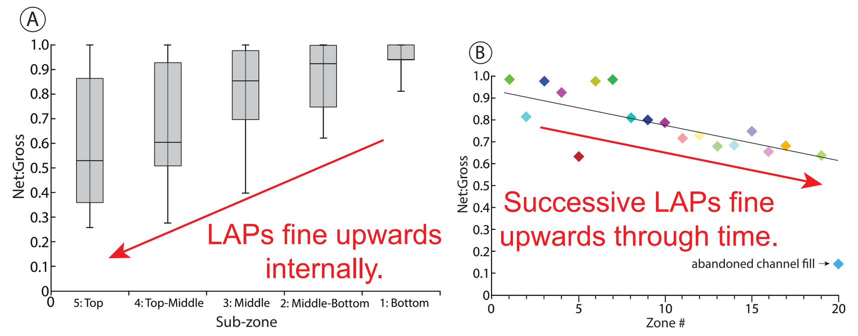

Figure 4.4: A) Box and whisker plots of net to gross (NTG) sand thickness by sub-zone. B) NTG by Zone. (Modified from Durkin et al., 2016)

Stratigraphic architecture and log data provide the basis for a series of statistical analyses. Vertical proportion curves (VPC) were calculated layer by layer for each zone and sub-zone. Horizontal proportion curves (HPC) represent the lateral changes in facies proportions from sub-zone to sub-zone within a zone. The statistics are incorporated into a 3D probability volume (which constrains simulations as soft conditioning): vertical proportions at each subzone were interpolated along layers to generate facies probabilities at all points throughout each zone.

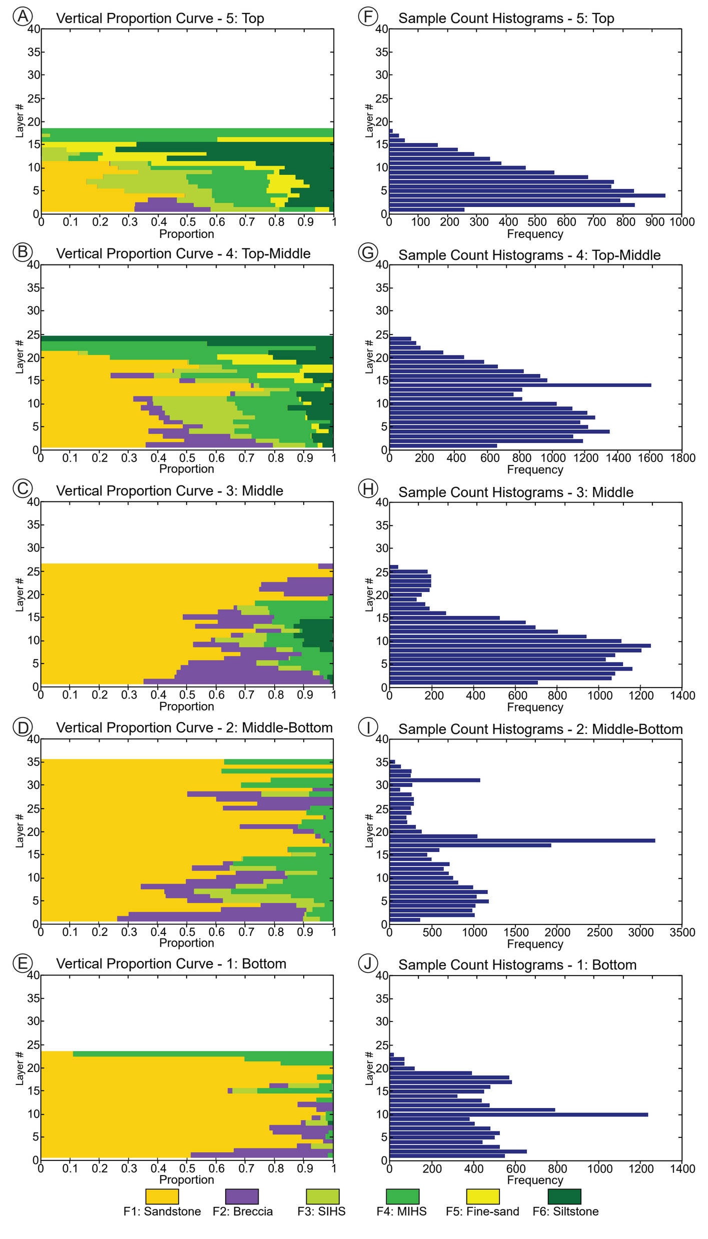

Figure 4.2: A)-E) Vertical proportion curves (VPC) by sub-zone, for all zones in the model. F)-J) with corresponding histograms. (Modified from Durkin et al., 2016)

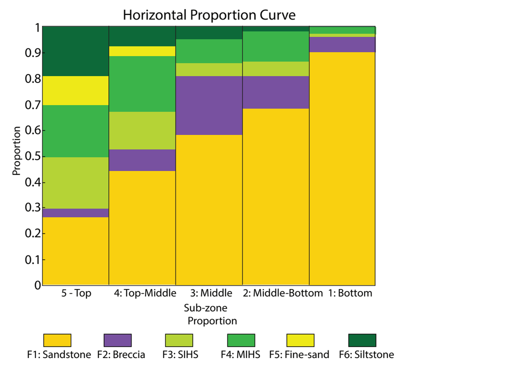

Figure 4.3:A) Global horizontal proportion curve (HPC) by sub-zone, for all zones in the geocellular model. (Modified from Durkin et al., 2016)

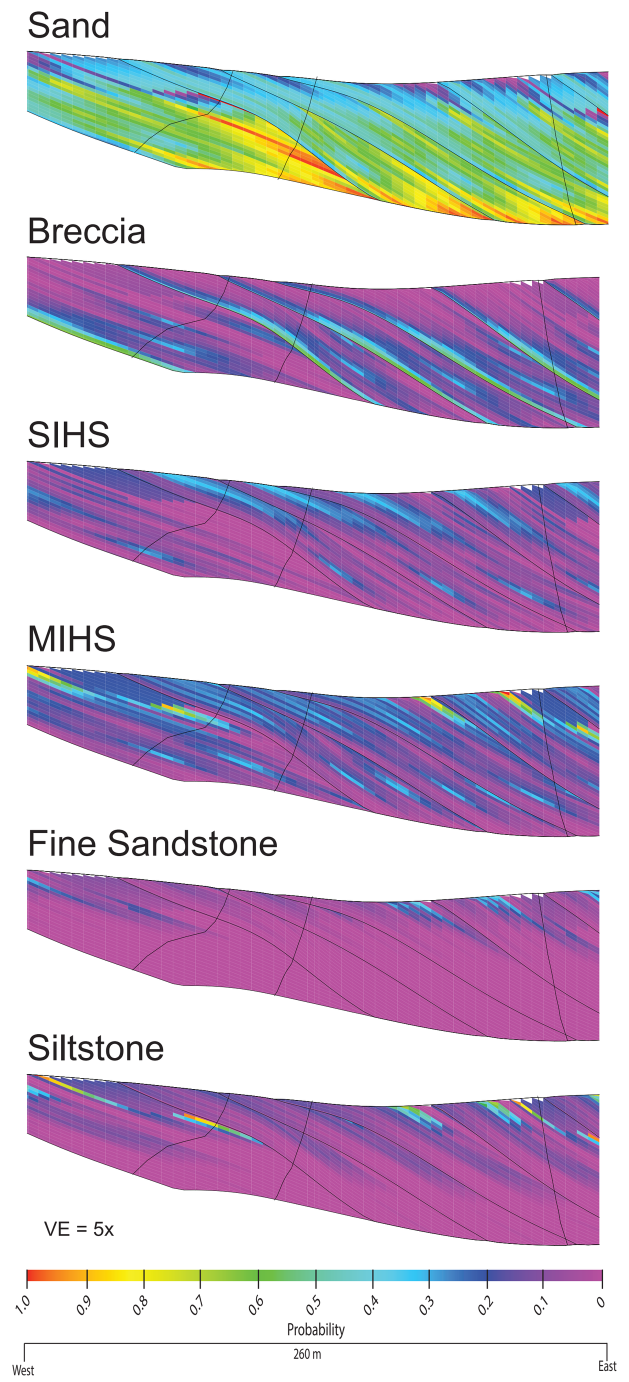

Figure 4.5: Probability Volumes for all facies visualized at sector model transect.

Vertical transition probabilities (VTP) were calculated using an embedded Markov-chain analysis where the vertical transitions from one facies to another are tallied and divided by the sum total of tallies in order to produce facies transition probabilities. Horizontal transition probabilities (HTP) were calculated using a spatial Markov chain along layers (out to 200 m). These data inform Lithotype Rule (LTR) construction for PGS. Complex transition probabilities are simplified to an LTR, which specifies order of facies transition in models.

5. 1-Dimensional Tests

2 Facies: Sequential Indicator Soft Data Experiment

Simple 1-D, 2 facies test illustrating the impact of 1) soft data probabilities, and 2) how soft data weight (Bz) informs facies distribution.

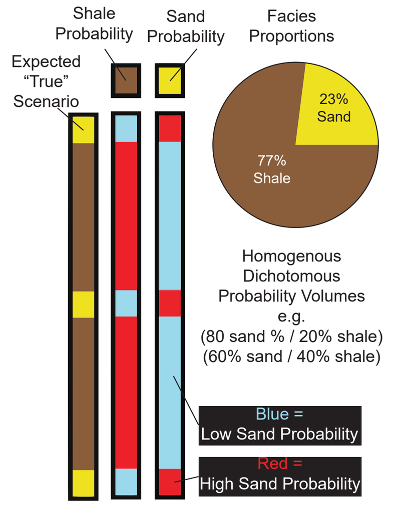

Bz Coefficient:
A measure of how well soft data distinguishes facies

For each facies:
Bz = E{P(Ik(soft(u)) | I(u;k) = 1} - E{P(Ik(soft(u)) | I(u;k) = 0}
ie. "Mean of soft data where given facies occurs" - "Mean of soft data where given facies does not occur"

e.g. Probabilities of 0.8 and 0.2 yield a Bz of 0.6 (given these cases are homogenous)

Probability of Misclassification:
A measure of how well models reproduce hard data

$$P_{misclass} = \frac{1}{n}\sum_{i=1}^{n}\left(1-\frac{c}{r}\right)$$

Where:
c = # of times correct facies simulated
r = # realizations
n = # of cells

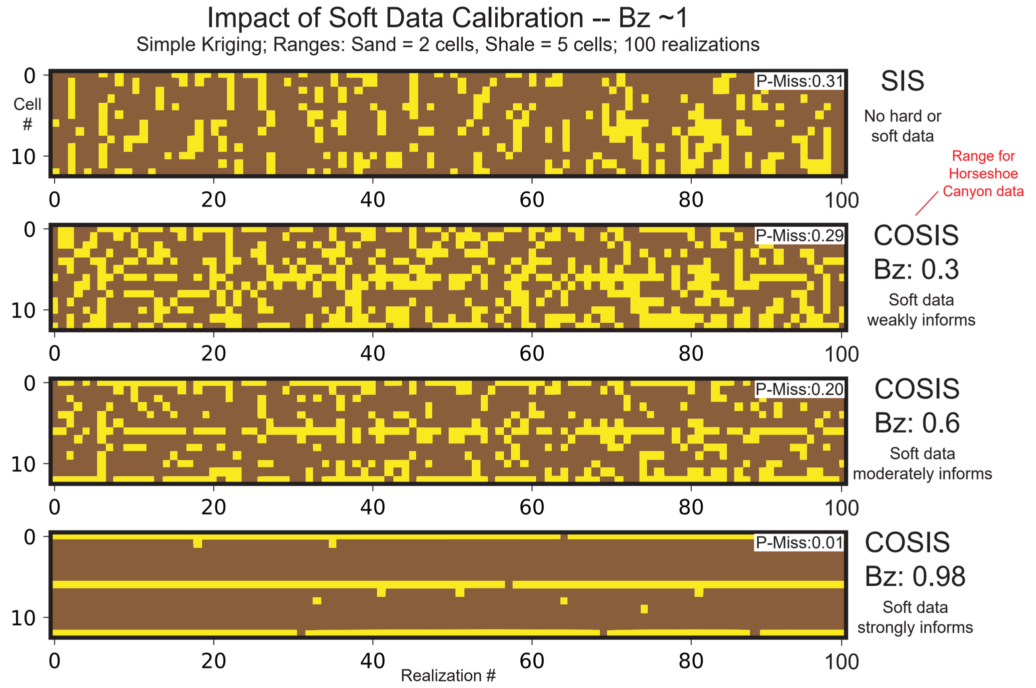

Figure 5.1: High- (shale) and moderate- (sand) proportion facies modeling tests were set up in a 13-cell 1-D grid with perfectly homogenous, dichotomous probability volumes (i.e. 0.8 and 0.2). Probability volumes were designed to reproduce an expected case, from which implicit Bz coefficients were calculated. High and low ***unconditional*** Bz scenarios were automated in SGeMS. Probability of misclassification, a measure of how well realizations reproduce hard data, was used to rank the impact of Bz and ranges of soft probabilities (decoupled for the sake of elucidating the impact of both parameters seperately).

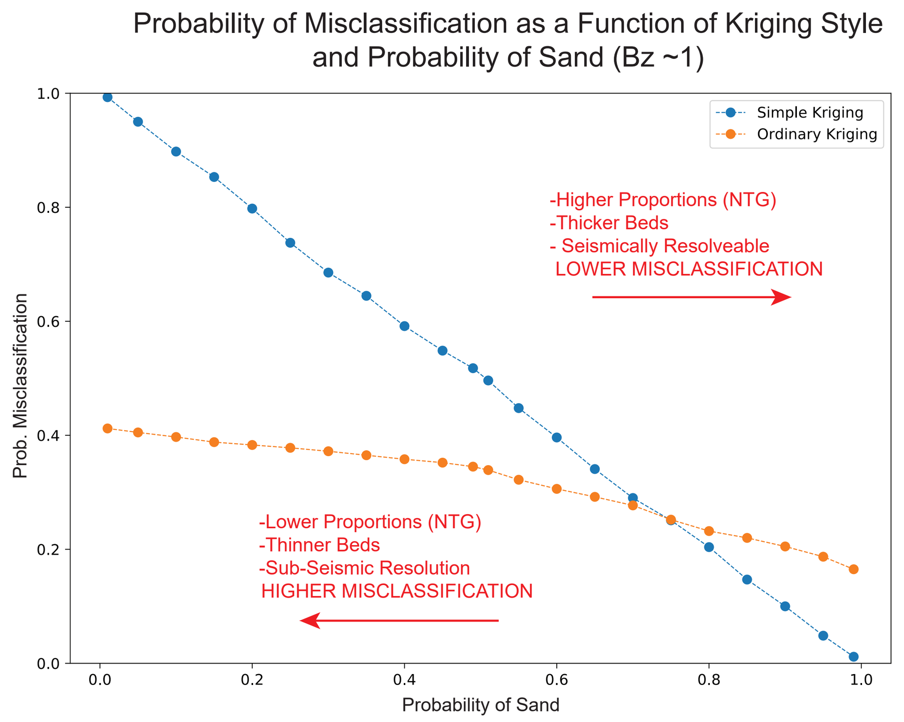

Figure 5.2: For a Bz =~ 1.0 (i.e., fully trusting the information content of soft probabilities) a decreasing probability of sand is linearly correlated to the probability of misclassification of sand. Conceptually, this relates back to seismic resolvability of thin beds. Whether a given facies is high-proportion or not, if it is not distinct in the soft data, it will be of little aid in guiding modeling. Simple Kriging appears to be a better predictor of facies than Ordinary Kriging when probabilities for a given facies are high (i.e. highly distinct), but is a weaker predictor of facies when probabilities are less distinct.

- Employing soft data with a low Bz (i.e., weak soft data conditioning) produces similar results to unconditioned SIS.
- Probability of Misclassification decreases significantly as a function of Bz, but varies whether simple or ordinary kriging is employed.

3 Facies: Characterizing Horseshoe Canyon Data

Testing the probability of misclassification when more than 2 facies are present in lower proportions. The hypothesis is that the ability to accurately predict facies will decrease with increasing number of facies.

- Probabilities (Fig 4.5) and measured section facies (upscaled to grid) were extracted along log 24 (see Figure 2.1 for location).
- Three facies were simulated (sand, breccia, and grouped fine-grained facies) to test the impact of 3 facies and the "real data" in a simplified 1D test.
- COSIS was run with different degrees of hard data conditioning (hard data %) to test the relative impacts of hard and soft data facies prediction.

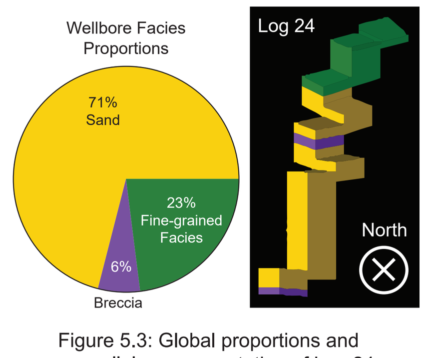

Figure 5.3: Global proportions and geocellular representation of Log 24.

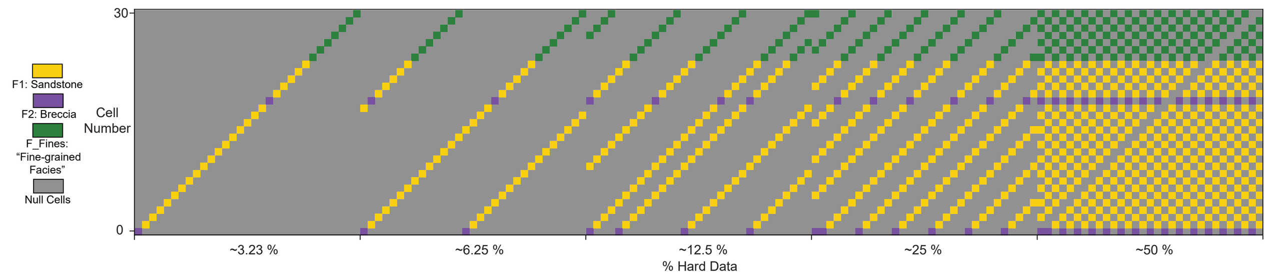

Figure 5.4: Hard Data Scenarios extracted from Log 24. 156 hard-data scenarios were tested: 31 at each of 5 different percent-cases and one with no hard data.

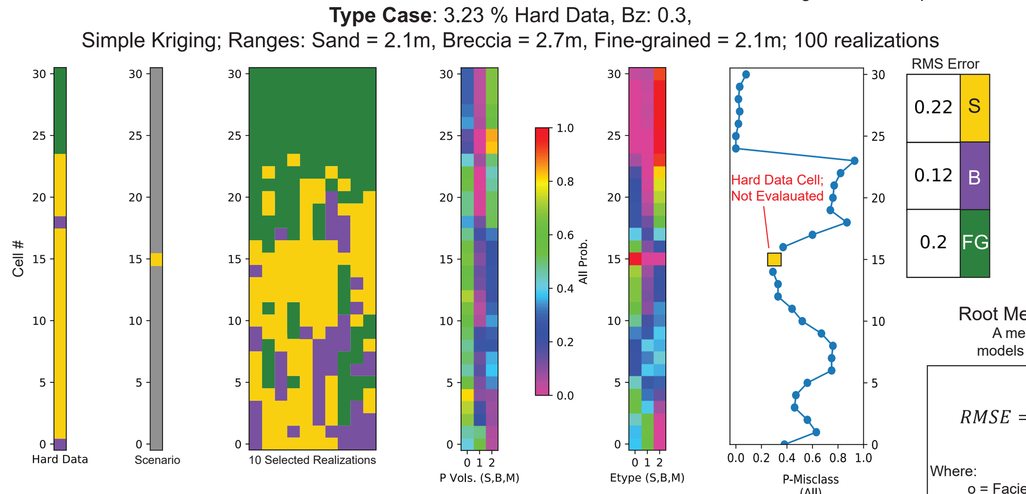

Root Mean Squares Error
A measure of how well models reproduce soft data

$$RMSE = \sqrt{\frac{1}{n}\sum_{i=1}^{n}(o-p)^2}$$

Where:
o = Facies E-type value
p = Facies Probability Volume value
n = # of cells

Figure 5.5: Type Realization and Summary Charts. For dozens of parameterizations of each hard data scenario, hundreds of SIS realizations were automated with SGeMS. Realization Root Mean Squares Error data was collected by comparing an E-Type for each facies to the probability volume, and Probability of Misclassification was calculated from the true hard data. Each is a proxy for realization fidelity to soft or hard data, respectively.

- Increased hard data % reduces probability of misclassification (i.e., better reproducing "true" facies distribution, excepting breccia), but increases RMSE (i.e., soft data mismatch).
- Soft data, as generated from VFPs, may help drive facies distribution when constrained to well data in the full field model. When soft data weight is low, the soft probabilities have less impact on facies distribution where as hard data % has a stronger impact (and vice versa when soft data weight is high).
- **Low-proportion facies are not reliably reproduced by SIS, with or without incorporating soft data.**

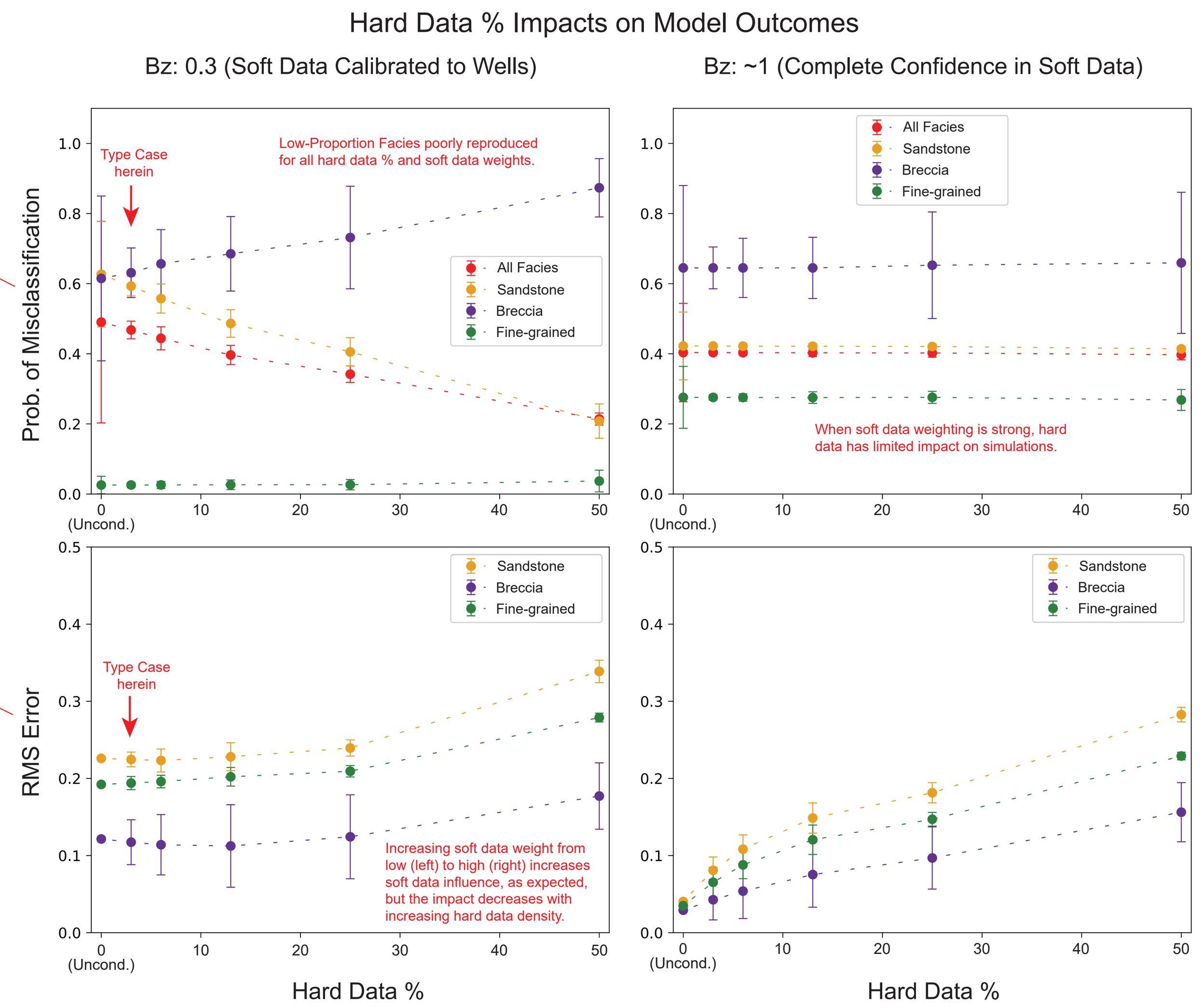

6. Results & Problems: TGS & PGS

Variogram-based methods were tested for their ability to reproduce facies architecture at the bed-scale. Utilizing a small sector model allows rapid testing of multiple parameterizations.

Co-Sequential Indicator Summary

Parameters
Variography
-Hz -- Sand : 100m, Breccia: 300m; 600m for Fine-grained
-Vt -- 0.3m for all facies (emphasizing lateral continuity)

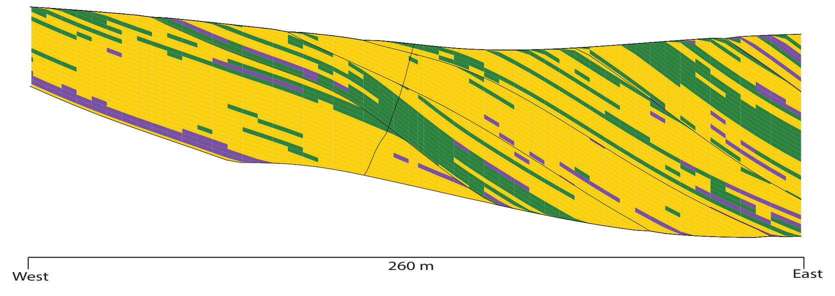

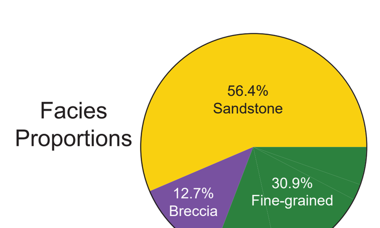

Figure 6.1: COSIS Characteristic Realization

- Employs variography to characterize each facies' spatial correlation independently.
- Leverages VPC through probability volume, but does not make direct use of VTP/HTP.
- Honors input variography and proportions (NOTE: this is a 3-facies case).
- Reproduces some outrop essence, but bedding is intermittent.

Truncated Gaussian Summary

Parameters
Variography
-Hz -- Sand : 100m, Breccia: 300m; 600m for all others
-Vt -- 0.3m for all facies (emphasizing lateral continuity)

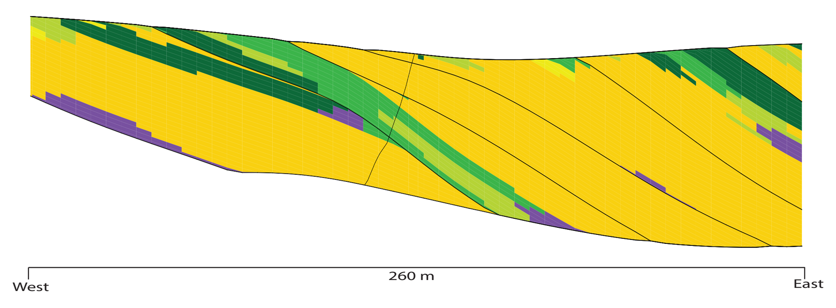

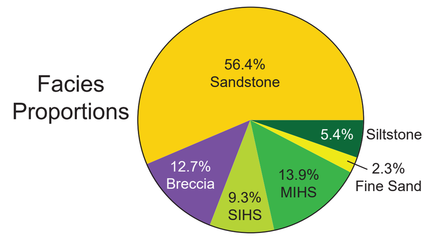

Figure 6.2: TGS Characteristic Realization

- Nested, hierarchical facies simulation that can employ variography to characterize each facies' spatial correlation independently.
- Leverages VPC through probability volume, but does not make direct use of VTP/HTP.
- Honors input variography and proportions.
- Reproduces some outrop essence: Breccias are associated with LAP bases and lower-energy facies increase up-section. Smooth transitions between facies packages.
-This realization incorporates minor smoothing.

Plurigaussian Summary

Parameters
Variography
-Hz -- 150m for both transition set
-Vt -- 0.3m for both transition sets (emphasizing lateral continuity)

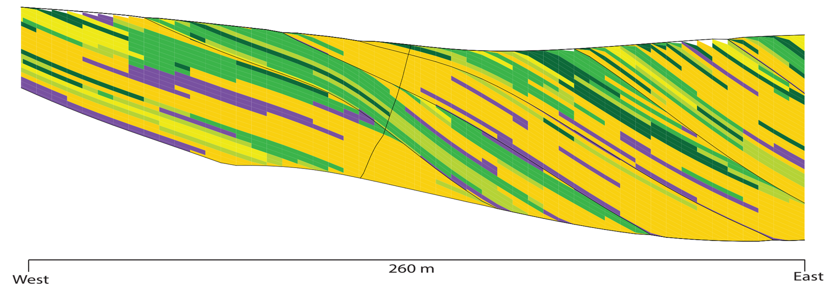

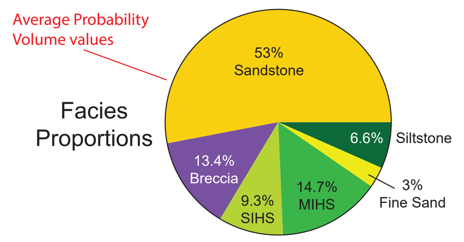

Figure 6.3: PGS Characteristic Realization

- Limited to two variograms per transition set to characterize all facies transition behavior and spatial correlation.
- Leverages VPC through probability volume, and approximates VTP/HTP through simplified LTR scheme.
- Honors input variography and proportions.
- Lower-quality reproduction of outcrop essence: facies length-scales and transitions are too variable and chaotic, leading to disorderly realizations.

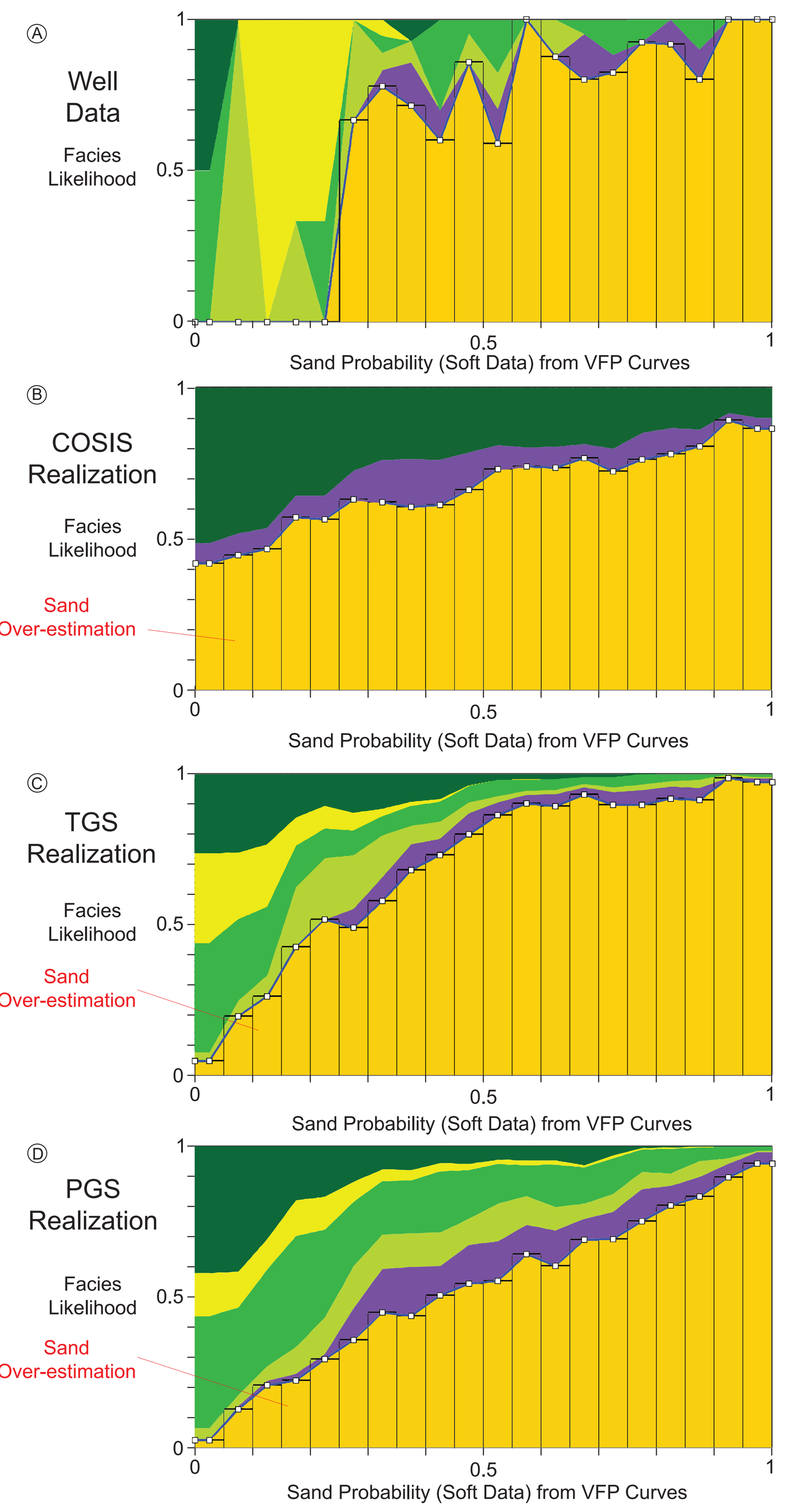

Figure 6.4: Likelihood of finding a particular facies in a data-set given a particular soft data (i.e. VFP) sandstone probability for A) Wells Data, B) COSIS, C) TGS, and D) PGS realizations. COSIS, TGS, and PGS over-populate sandstone at locales with low sandstone probabilities as compared to well data.

- Sand is over-populated in realizations where sand probabilities are low (compare graphs from models to well data above). Low sand probabilities in Fig 6.4 A represent tops of point bars, which are filled predominantly by fine-grained facies. Fig. 5.4 B to D show that all methods are populating sands in these low probability zones where they should not be.

- The implication is that you are creating more flow across point bar tops and decreasing flow across bottoms.

7. Problems with Variogram-based Modeling

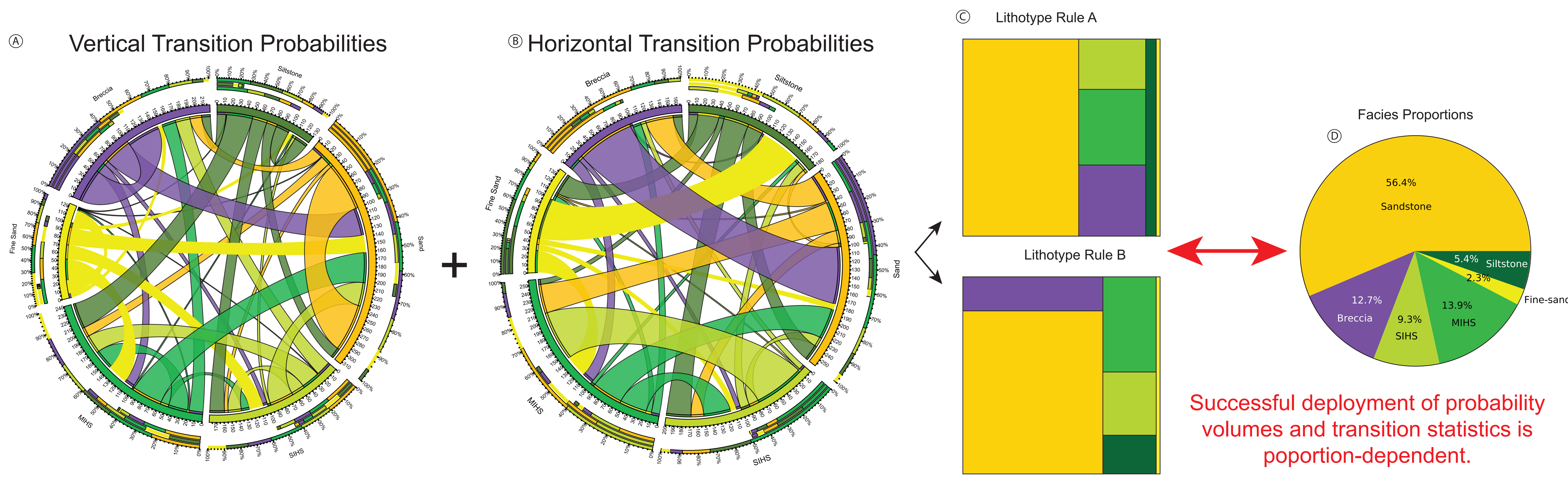

Figure 7.1: A) Vertical and B) Horizontal transition probabilities visualized as Circos diagrams (Circos Table Viewer, 2017) where colored bands represent probability of transition between given facies. C) For PGS, these complex facies-transition relationships must be simplified into Lithotype Rules (LTR) that enforce order of occurrence and transition between facies (e.g. in LTR B, Breccia must lie adjacent to Sand or MIHS). These LTR examples are symbolic of the mean probability of each facies' probability volume and D) correspondingly the true measured facies proportions.

- Variogram-based modeling sometimes under-represents low-proportion facies.

- PGS and nested, heierarchical TGS adequately reproduce low-proportion facies in realizations.

- Low-proportion facies are baffles and barriers to flow that are important to represent correctly.

- PGS and TGS do not appear to adequately reproduce architecture of low-proportion facies. While we hypothesized that transition statistics could enforce architectural outcomes, Lithotype Rules over-simplify transition probabilities when facies are numerous, and/or given facies are low-proportion, resulting in sub-obtimal realizations.

8. Training Image-Based Modeling

Given the limits of variogram-based modeling, pattern-based modeling may hold the key to bed-scale architecture reproduction through training images development via outcrop statistics.

Candidates Include:

- Deterministic training images derived from outcrop photopans (see Figure 3.1).
- SNESIM Widely deployed MPS algorithm.
- FILTERSIM FILTERSIM can utilize conventional categorical training images, but because FLITERSIM can utilize continuous training images, there is space to experiment with the probability volumes directly.

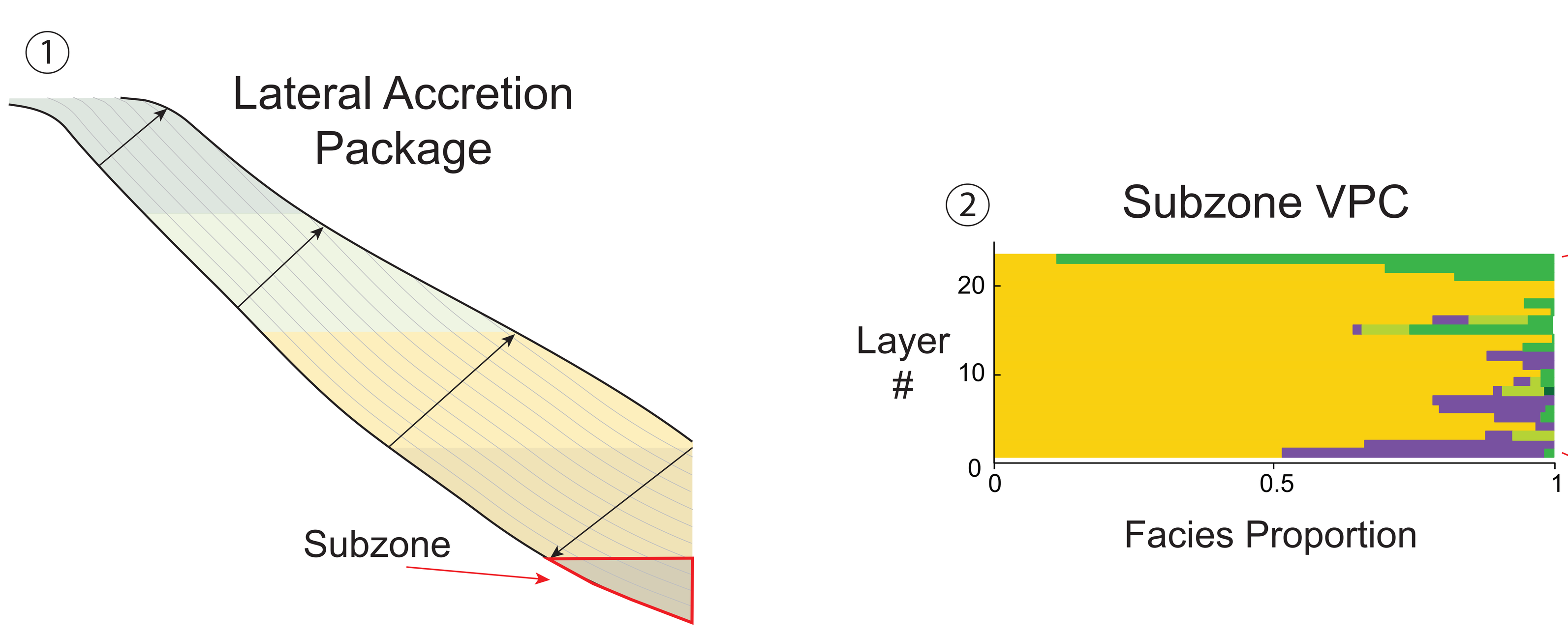

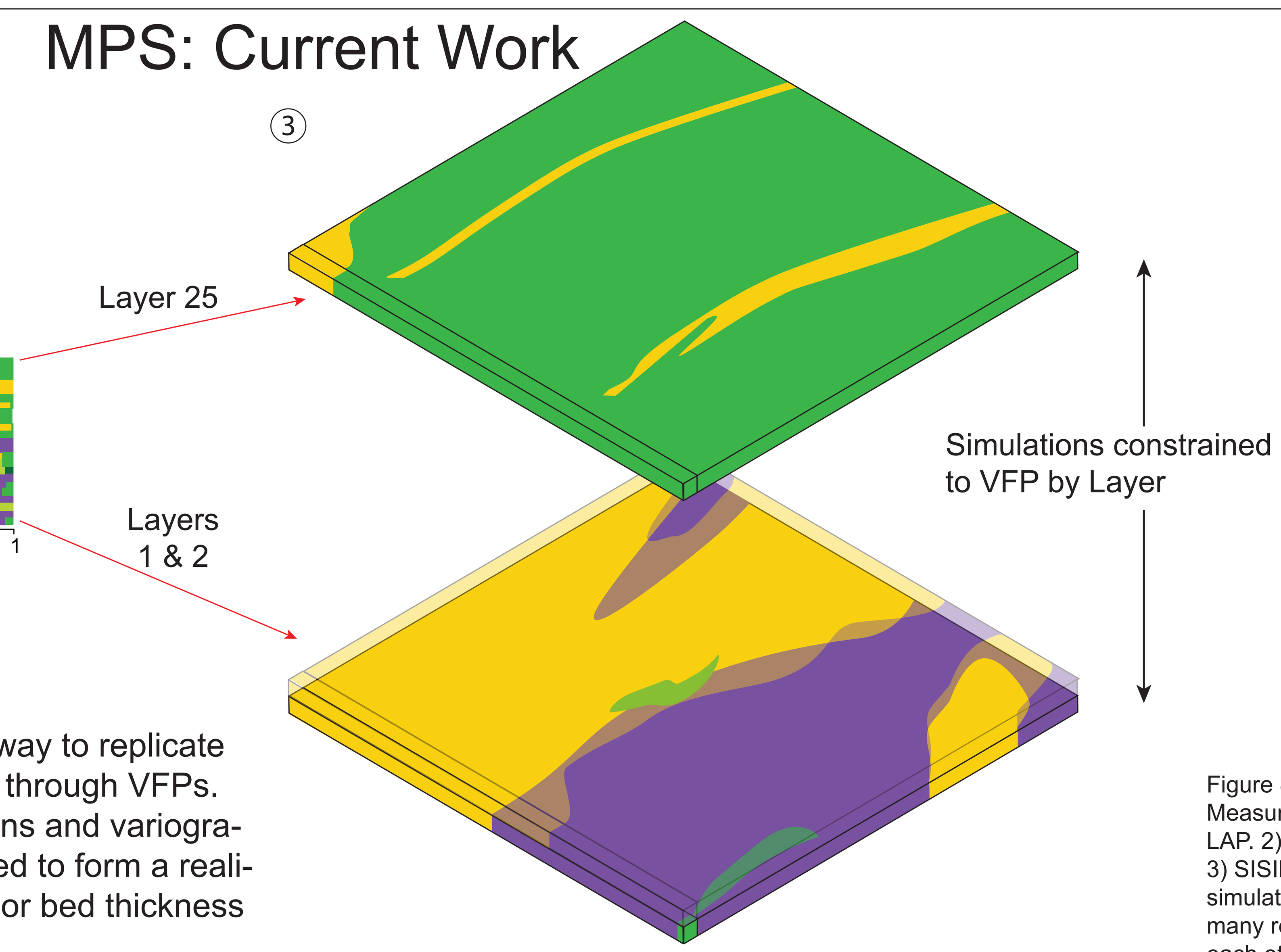

④ OUTPUT:
Training Image, Composite from many Realizations

Deriving training images (TI) from bed-scale outcrop statistics may prove a powerful way to replicate geologic essence in models. Each layer in a LAP is characterized, for each subzone, through VFPs. Sequential Indicator Simulations (SISIM) run for each layer, with only facies proportions and variography as constraint (and the preceding layer-realization as soft condition) can be stacked to form a realization of the subzone. Many such 'stacks' could be screened for realizations that honor bed thickness and transition probabilities, and then aggregated into a zonal TI.

Figure 8.1: Statistically-infused Training Image Generation Concept. 1) Measured section data is broken into subzones based on position in each LAP. 2) The VPC for each subzone breaks out facies proportions by layer. 3) SISIM constrained to layer facies proportions can be stacked into a single simulated volume representing the subzone statistics. 4) The composite of many realized volumes could be chained to comparable composites from each other subzone to build a TI.

9. Conclusions

-COSIS, even with strong soft conditioning, may have difficulty reproducing proportions of facies where the target-proportion is low.

- TGS and PGS reproduce facies proportions correctly, but do not appear to reproduce architecture adequately.

- Pattern-based modeling algorithms will be explored as an option to reproduce bed-scale facies architecture.

10. Acknowledgements

I would like to thank Schlumberger and Geovariances for supplying software to facilitate this modeling effort. I would also like to thank fellow Geomodeling Research Group students, Adam Nielson, Casey Meirovitz, and Heather Judd for their support, insight and feedback throughout this process. Finally, I would like to thank Dr. Lisa Stright, Dr. Paul Durkin, and Dr. Stephen Hubbard for the opportunity to work on this dataset. Support for Rocks2Models projects comes from ConocoPhillips Corporation, Royal Dutch Shell PLC, and Hess Corporation. Additionaly, fieldwork for this study was supported by ConocoPhillips Canada and CNOOC Nexen Inc. Field assistance was provided by Dustin Bauer, Ross Kukulski, Sean Fletcher, Ben Daniels, Aaron Reimchen and Tore Klausen.

11. References

Ainsworth, R.B., 1994, Marginal marine sedimentology and high-resolution sequence analysis; Bearpaw -Horseshoe Canyon transition, Drumheller, Alberta: Bulletin of Canadian Petroleum Geology, v. 42, p. 26–54.
Ainsworth, R.B., Vakarelov, B.K., Lee, C., MacEachern, J.A., Montgomery, A.E., Ricci, L.P.and Dashtgard, S.E., 2015, Architecture and evolution of a regressive, tide-influenced marginal marine succession, Drumheller, Alberta, Canada: Journal of Sedimentary Research, v. 85, p. 596-625.
Burgess, P.M., 2016, Identifying ordered strata: Evidence, methods, and meaning. Journal of Sedimentary Research, v. 86, p. 148-167.
Deschamps, R., Guy, N., Preux, C., and Lerat, O., 2013, Analysis of heavy oil recovery by thermal EOR in a meander belt: From geological to reservoir modeling. Oil and Gas Science Technology, v. 67, p. 999-1018.
Durkin, P. R., Hubbard, S. M., Boyd, R. L., and Leckie, D. A., 2015, Stratigraphic expression of intra-point-bar erosion and rotation. Journal of Sedimentary Research, v. 85, p. 1238-1257.
Durkin, P. R., Stright, L., Hubbard, S. M., 2016, Statistical Analysis of An Outcropping Point Bar Deposits Informs Construction of Geologically Realstic 3D Geocellular Models,Geological Society of America Abstracts with Programs v. 48, n. 7.
Eisbacher, G.H., Carrigy, M.A., and Campbell, R.B., 1974, Paleodrainage pattern and late orogenic basins of the Canadian cordillera: in Dickinson, W.R., ed., Plate Tectonics and Sedimenation: SEPM, Special Publication 22, p. 143-166.
Ethier, V. G., 1975, Application of Markov analysis to the Banff Formation (Mississippian), Alberta. Journal of the International Association for Mathematical Geology, v. 7, p. 47-61.
Forzoni, A., Hampson, G., and Storms, J., 2015, Along-strike variations in stratigraphic architecture of shallow-marine reservoir analogues: Upper Cretaceous Panther Tongue delta and coeval shoreface, Star Point Sandstone, Wasatch Plateau, Central Utah, USA. Journal of Sedimentary Research, v. 85, p.968-989.
Fustic, M., Thurston, D., Al-Dliwe, A., Leckie, D. A., and Cadiou, D., 2013, Reservoir modeling by constraining stochastic simulation to deterministically interpreted three-dimensional geobodies: Case study from Lower Cretaceous McMurray Formation, Long Lake steam-assisted gravity drainage project, northeast Alberta, Canada. in F. J. Hein, D. Leckie, S. Larter, and J. R. Suter, eds., Heavy-oil and oil-sand petroleum systems in Alberta and beyond: AAPG Studies in Geology 64, p. 565–604.
Hamblin, A.P., 2004, The Horseshoe Canyon Formation in southern Alberta: Surface and subsurface stratigraphic architecture, sedimentology, and resource potential: Geological Survey of Canada Bulletin 578, 180 p.
Hampson, G. J., Gani, M. R., Sharman, K. E., Irfan, N., and Bracken, B., 2011, Along-strike and down-dip variations in shallow-marine sequence stratigraphic architecture: Upper Cretaceous Star Point Sandstone, Wasatch Plateau, Central Utah, USA. Journal of Sedimentary Research, v. 81, p. 159-184.
Lavigne, J., 1999, Aspects of marginal marine sedimentology, stratigraphy and ichnology of the Upper Cretaceous Horseshoe Canyon Formation, Drumheller, Alberta: M.Sc. Thesis, University of Alberta, Edmonton, Alberta, 146 p.
Leckie, D.A., and Smith, D.G., 1992, Regional setting, evolution, and depositional cycles of the Western Canada Foreland Basin; in Macqueen, R.W., and Leckie, D.A., eds., Foreland Basins and Fold Belts: American Association of Petroleum Geologists, Memoir 55, p. 9-46.
Leeder, M., 2011, Chapter 11, Rivers, in Sedimentology and Sedimentary Basins: From Turbulence to Tectonics, Second Edition, p. 245-281.
Li, H., and White, C. D., 2003, Geostatistical models for shales in distributary channel point bars (Ferron Sandstone, Utah): From ground-penetrating radar data to three-dimensional flow modeling. American Association of Petroleum Geologists bulletin, v. 87, p. 1851-1868.
Miall, A. D., 1973, Markov chain analysis applied to an ancient alluvial plain succession. Sedimentology, v. 20, p. 347-364.
Moreton, D., Carter, J., Peacock, M., and Rogala, B., 2013. Athabasca oil sands: Application of integrated technology in the identification of commercial thermal and mining opportunities: International Petroleum Technology Conference, Beijing, China, 26-28 March 2013.
Nardin, T.R., Feldman, H.R., and Carter, B.J., 2013, Stratigraphic architecture of a large-scale point-bar complex in the McMurray Formation: Syncrude's Mildred Lake Mine, Alberta, Canada, in Hein, F.J., Lecke, D., Larter, S., and Suter, J.R., eds., Heavy-Oil and Oil-Sand Petroleum Systems in Alberta and Beyond: American Association of Petroleum Geologists, Studies in Geology 64, p. 273-311.
Rahmani, R.A., 1988, Estuarine tidal channel and nearshore sedimentation of a Late Cretaceous epicontinental sea, Drumheller, Alberta, Canada, in de Boer, E.L., van Gelder, A., and Nio, S.D., eds., Tide-Influenced Sedimentary Environments and Facies: First Edition, p. 433-471.
Ravenne, C., Galli, A., Doligez, B., Beucher, H., & Eschard, R., 2002. Quantification of facies relationships via proportion curves. In Geostatistics Rio 2000: Springer Netherlands, p. 19-39.
Schwarzacher, W., 1969, The use of Markov chains in the study of sedimentary cycles. Journal of the International Association for Mathematical Geology, v. 1, p. 17-39.
Shepheard, W.W., and Hills, L.V. 1970, Depositional environments Bearpaw – Horseshoe Canyon (Upper Cretaceous) transition zone Drumheller "Badlands", Alberta: Bulletin of Canadian Petroleum Geology, v. 18, p.166-215.
Su, Y., Wang, J. Y., and Gates, I. D., 2013, SAGD well orientation in point bar oil sand deposit affects performance. Engineering Geology, v. 157, p. 79-92.